STRUCTURAL AND FUNCTIONAL STUDIES OF THE EARLY T LYMPHOCYTE ACTIVATION 1 (*Eta-1*) GENE

Definition of a Novel T Cell-dependent Response Associated with Genetic Resistance to Bacterial Infection

By R. PATARCA, G. J. FREEMAN, R. P. SINGH, F.-Y. WEI, T. DURFEE,* F. BLATTNER,* D. C. REGNIER,‡ C. A. KOZAK,§ B. A. MOCK,‖ H. C. MORSE III,‡ T. R. JERRELLS,¶ AND H. CANTOR

*From the Laboratory of Immunopathology, Dana-Farber Cancer Institute, Department of Pathology, Harvard Medical School, Boston, Massachusetts 02115; the *University of Wisconsin, Madison, Wisconsin 53706; the ‡Laboratory of Immunopathology; and the §Laboratory of Molecular Microbiology, National Institute of Allergy and Infectious Disease; and the ‖National Cancer Institute, National Institutes of Health, Bethesda, Maryland 20892; and the ¶University of Texas Medical Branch, Galveston, Texas 77550*

There is considerable evidence for genetic control of resistance to infections by bacteria, viruses, and protozoa (1). One class of genes confers resistance by nonimmunological mechanisms. Notable examples are the Duffy and *Mx* genes, which affect resistance to *Plasmodium vivax* and influenza virus, respectively (2, 3). A second class of genes that may confer resistance by immunological mechanisms has been inferred from the responses of inbred mice to a variety of infectious agents (1). However, with the exception of loci in the MHC (1), the relevant genes and their products have escaped molecular definition. We have approached this problem by molecular cloning and analysis of genes that map to loci involved in regulation of immune responses. This approach led previously to the description of the regulatory protein T lymphocyte 1 (*Rpt-1*)[1] gene, which encodes an intranuclear protein that inhibits expression of the human HIV-1 in T cells (4).

In this report, we describe a murine cDNA, designated early T lymphocyte activation 1 (Eta-1), which maps to a locus that confers genetic resistance to infection by bacteria responsible for human scrub typhus (5). The *Eta-1* gene encodes a very acidic secreted protein that has structural features associated with binding to cell adhesion receptors. Studies of the cellular expression of *Eta-1* suggest that it marks a rapid T cell-dependent response to bacterial infection that may be associated with host resistance.

This work was supported by National Institutes of Health grants AI-12184, AI-13600, and CA-26695 to H. Cantor; AI-27858 to T. R. Jerrells; GM-21812 to F. Blattner; an American Cancer Society postdoctoral fellowship to G. J. Freeman; and a Cancer Research Institute/Geist Foundation postdoctoral fellowship to R. P. Singh.

[1] *Abbreviations used in this paper:* Eta-1, early T lymphocyte activation 1; GAPDH, glyceraldehyde 3-phosphate dehydrogenase; PFU, plaque-forming units; RDU, relative densitometric units; RI, recombinant inbred; Rpt-1, regulatory protein T lymphocyte 1, RT, *Rickettsia tsutsugamushi.*

Materials and Methods

Mice and DNA Samples. All inbred mouse strains listed in Table II were obtained from colonies at the National Institutes of Health, Bethesda, MD, the Jackson Laboratory, Bar Harbor, ME, or the Netherlands Cancer Institute. (CBA/J × C57BL/6)F_1 *nu/nu* mice and euthymic littermates were kindly provided by Dr. H. H. Wortis, Tufts University School of Medicine, Boston, MA. DNA samples from BXH recombinant inbred strains were purchased from the Jackson Laboratory and the CXS recombinant inbred strains were a gift from Dr. J. Hilgers, Academisch Kiekenhuis Vrige Universiteit, Amsterdam.

Cloned T Cells and Lymphocyte Subpopulations. Enrichment of T cells was obtained after passage of spleen cells through nylon wool columns (6), and depletion of T cells was obtained using anti-Thy-1, anti-Ly-1, and Ly-2 antibody with a source of rabbit complement as described previously (7). The derivation, characterization, and maintenance of the T cell clones used in this report have been described previously (7–9). Briefly, Cl.Ly1T1, Cl.Ly1-N5, and Cl.Ly1-S1 are Th cell clones, and Cl.NK-11 is an NK cell clone. Cells were considered to be in the resting state when they ceased to proliferate in response to conditioned medium 2–4 wk after antigenic stimulation.

Production of a T Cell-specific cDNA Probe and Library. The cDNA library was constructed as described previously (4). Briefly, poly(A)$^+$ RNA from Cl.Ly1-T1 (22 h after activation) was used to prepare a cDNA library of 3.8×10^5 clones in the pcD vector (10). A size-selected sublibrary of ~9,800 clones (inserts from 0.5 to 20 kb) was sparsely plated onto agar plates (11), replica plated onto nitrocellulose filters, amplified by chloramphenicol treatment, and prepared for hybridization. Colonies hybridizing to a T cell-specific cDNA probe (4) were further analyzed by restriction enzyme digestion, crosshybridization, and Northern blot analysis using RNA from B cell lines, resting, and activated T cells (12). The nucleotide sequence of the cDNA insert was determined by the procedure of Maxam and Gilbert (13) and Northern blot analysis was performed as described (12, 15).

Southern Blot Analysis and Somatic Cell Hybridization. Genomic DNA from inbred mouse strains was digested with Eco RV and Xba I, analyzed on agarose gels, transferred to nitrocellulose filters, and hybridized to a ^{32}P-labeled, nick-translated Hae III fragment of *Eta-1* cDNA (14). Somatic cell hybrids used for chromosomal localization of *Eta-1* were produced by fusion of Chinese hamster cell line E36 with murine cells (16), and DNA from these cells was digested with Eco RI, run on agarose gels, transferred to filters, and hybridized to the Hae III *Eta-1* cDNA probe as described (16).

Transfections. 10^6 COS-7m6 cells (an SV40 T antigen-positive monkey kidney epithelial cell line) per dish supplemented with 10 ml DMEM, 10% FCS were transfected with 6 μg of plasmid DNA as described (17). Dishes were incubated at 37°C in 5% CO_2 for 48 h. The media was replaced every 24 h. To obtain biosynthetically labeled supernatant fluid proteins, after 48 h cells were incubated for 3 h in DME lacking methionine, and subsequently for 6 h with 25 μCi/ml ^{35}S-methionine. The supernatant fluids were collected and centrifuged at 100,000 *g* for 60 min to remove cellular debris.

Analysis of Proteins in Supernatant Fluids of Transfected COS-7m6 Cells. A modification of the method of O'Farrel (18) was used to allow high resolution of biosynthetically labeled proteins in unfractionated COS-7m6 supernatant fluids. Briefly, 1.5×10^5 cpm of ^{35}S-methionine-labeled proteins were loaded onto an isoelectric focusing tube gel (pH 3–10, 1.0 × 110 mm) from the cathodic end, and focused for 2.5 h at 400 V. The time for the nonequilibrium pH gradient electrophoresis was reduced to 1.5–2 h from 6 h to allow resolution of acidic proteins before size analysis. After electrophoresis in the first dimension, the gels were cut into 10-mm slices and equilibrated for 40 min in SDS sample buffer (0.06 M Tris-HCl, pH 6.8, 2% SDS, 5% β-mercaptoethanol, 10% glycerol) before loading onto 10% SDS-PAGE, and subjected to electrophoresis at 30 mA for 5 h. Gels were fixed and soaked in Entensify (New England Nuclear, Boston, MA) before autoradiography with Kodak-X-AR film for 5 d.

Analysis of Eta-1 Expression In Vivo. Con A (Sigma Chemical Co., St. Louis, MO) was administered intraperitoneally (10 μg/mouse in 0.2 ml PBS). CFA (Gibco Laboratories, Grand Island, NY) containing 500 μg/ml killed *Mycobacterium bovis* in mineral oil was injected intraperitoneally (0.2 ml/mouse). The Gilliam strain (165th passage) of *Rickettsia tsutsugamushi* (RT) was propagated and titered as described (19). Mice were inoculated with 10^3 plaque-

forming units (PFU) using irradiated L929 cells; 1 PFU is sufficient to cause lethal infection of the *Ric*^{S} mouse strain C3H/Dub (19).

cDNA probes to *Eta-1* and *IFN-γ* (*Ifg*) hybridized to a single species of RNA according to Northern blot analysis (Fig. 1 and reference 4), and the levels of gene expression quantitated by densitometric measurement of Northern blots were the same as levels obtained by slot blot analysis. We used the latter technique to facilitate analysis of large numbers of samples. Peritoneal cells from three to five mice inoculated intraperitoneally with mitogen, CFA, or after infection with 10^3 LD_{50} U of RT were collected for each RNA sample. In experiments using mice carrying the *nu/nu* mutation, mesenteric lymph node cells were combined with peritoneal cells to obtain sufficient amounts of RNA for measurement.

After extraction of cellular RNA by the guanidine isothiocyanate method with cesium chloride modification (20), the amount of RNA in each sample was estimated by determining its absorbance at 260 nm (OD_{260}). 20-μg aliquots of RNA from each cellular sample were blotted onto nitrocellulose filters using a Minifold II slot blotter (Schleicher & Schuell, Inc., Keene, NH) and hybridized to ^{32}P-labeled cDNA corresponding to murine *Ifg* (4), *Eta-1*, and glyceraldehyde 3-phosphate dehydrogenase (*GAPDH*). *GAPDH* is expressed in all cells at levels that do not vary after cellular activation (20).

After preflashing, films were exposed and the intensity of radioactivity of the autoradiograms was quantitated using an Ultroscan II laser densitometer (LKB Instruments, Inc., Gaithersburg, MD), adjusting exposure times so that the intensity of autoradiographic signals corresponded to the linear range of densitometric detection. To ensure that the variation in the intensity of radioactive signals among different samples was independent of the fragment of cDNA probe used for hybridization, two fragments were separately used for *Eta-1*: an Xho I fragment containing the whole cDNA insert and an Hae III fragment spanning the 3′ coding region (Fig. 2 *A*).

To ensure that comparisons of Eta-1 and Ifg RNA levels in different cellular samples were based upon the same amount of RNA in each sample, the area under the densitometric peak for Eta-1 and Ifg for each cellular RNA sample was divided by the area under the GAPDH densitometric peak for the same cellular RNA sample. The ratios of test RNA to *GAPDH* RNA for each cellular sample are referred to as relative densitometric units (RDU) in the text.

Results

We derived a cDNA library (3.8×10^5) from an activated T cell clone (C1.Ly1-T1). About 10^4 colonies from this cDNA library were screened using a T cell cDNA probe from which B cell and fibroblast messages had been subtracted. After removal of colonies that hybridized with cDNA representing known lymphokines (e.g., IL-2, IL-3, IFN-γ), analysis of the remaining colonies (~400) showed that ~60 contained the same insert according to crosshybridization and restriction digest analysis, and accounted for ~3.0% of the inserts in the activated T cell cDNA library.

The Xho I fragment corresponding to the abundant cDNA insert, designated *Eta-1*, was used as a probe for Northern analysis of the corresponding mRNA in different cell types (Fig. 1 *A*). Steady-state levels of Eta-1 mRNA were very low or undetectable in unstimulated Th clones (Fig. 1 *A*, lanes *a* and *c*) and increased substantially within 18 h after activation by Con A (Fig. 1 *A*, lanes *b* and *d*). Similar results were seen with the Thy-1$^+$Ly-2$^-$Ly-4$^-$ clone NK-11 (Fig. 1 *A*, lanes *e* and *f*). By contrast, no hybridization was detected to poly(A)$^+$ RNA from the mast cell clone MC-9 in the presence or absence of Con A (Fig. 1 *A*, lanes *g* and *h*), from the murine B cell tumor 2PK3 (Fig. 1 *A*,lane *i*) or, using the hybridization conditions described, from PHA-stimulated human peripheral blood lymphocytes (Fig. 1 *A*, lane *j*).

We asked if *Eta-1* was expressed in vivo or whether its rapid induction after activation was a special feature of lymphocytes after long term in vitro growth. Spleen, thymus (Fig. 1 *B*), lymph node, and peritoneal cells from adult mice (latter two not

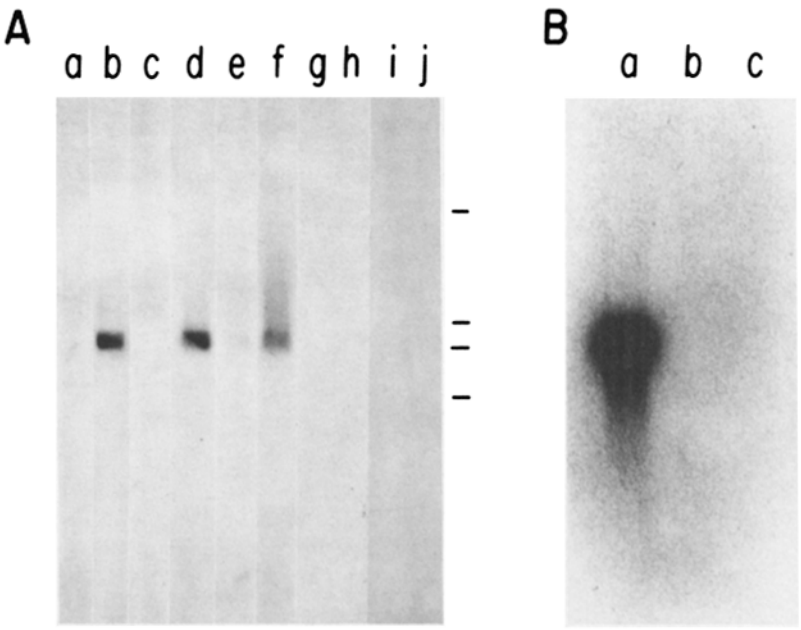

FIGURE 1. Northern analysis of *Eta-1* expression. (*A*) A ^{32}P-labeled 1.7-kb Xho I fragment containing the *Eta-1* cDNA insert from the pcD vector was hybridized to filters containing 5 μg of poly(A)$^+$ RNA (see Materials and Methods) from the following cells: (*a*) C1.Ly1-N5 (T_H clone); (*b*) C1.Ly1-N5 + Con A; (*c*) C1.Ly1-S1 (T_H clone); (*d*) C1.Ly1-S1 + Con A; (*e*) NK-11 (Thy-1$^+$ NK clone); (*f*) NK-11 + Con A; (*g*) MC.9 (mast cell clone); (*h*) MC.9 + Con A; (*i*) 2PK3 – B cell line; (*j*) human PBL + PHA. The RNA markers are indicated on the right and they correspond to 6, 1.765, 1.426, and 0.92 kb. (*B*) Overexposed Northern blot of 5 μg of poly(A)$^+$ RNA from: (*a*) C1.Ly1-T1 (T_H clone) + Con A; (*b*) thymocytes (from 10-wk-old C57BL/6 mice); (*c*) spleen cells (from 10-wk-old C57BL/6 mice).

shown) did not contain detectable levels of *Eta-1* RNA. However, cells from mice inoculated with an oil emulsion of killed *Mycobacterium bovis* (CFA) (Fig. 2 *A*) or the T cell mitogen Con A (Fig. 2 *B*) expressed substantial levels of *Eta-1* RNA within 24 h after stimulation.

Structure of Eta-1 cDNA and Predicted Eta-1 Protein. Fig. 3 shows the restriction pat-

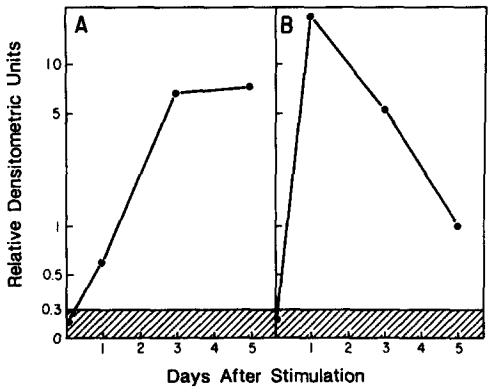

FIGURE 2. Slot blot analysis of steady state *Eta-1* RNA levels in peritoneal cells at the indicated times after intraperitoneal injection of 0.2 ml CFA (*A*) or 10 μg Con A (*B*). Relative densitometric units refers to the ratio of *Eta-1* to a control, noninducible RNA (*GAPDH*) for each cellular sample (see Materials and Methods for details). The hatched area indicates the mean +/– 2 SE of the relative densitometric units of *Eta-1* in peritoneal cells from mice injected with saline.

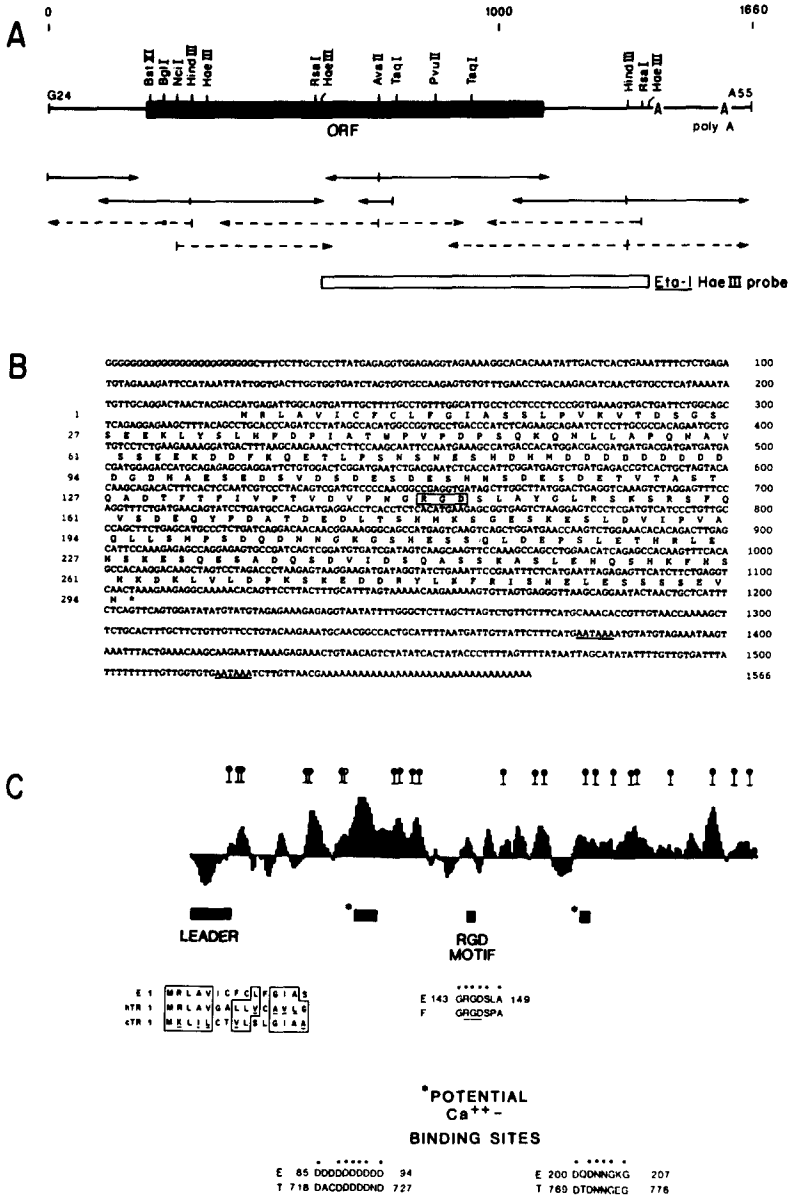

FIGURE 3. (*A*) Restriction endonuclease cleavage map of the cDNA insert of pcD-Eta-1. The coding region (ORF) is shaded in black. The arrows indicate the extent of sequencing done starting at the restriction sites indicated. Potential polyadenylation sites are denoted with the letter *A*. (*B*) Nucleotide and predicted amino acid sequence of *Eta-1*. The sequenced cDNA of 1,569 bp is shown. An open reading frame of 882 nucleotides (294 amino acids) is followed by a 3′ noncoding sequence that contains two potential polyadenylation sites, which are underlined. (*C*) Hydrophilicity plot of the predicted *eta-1* protein. A hydrophilicity plot for Eta-1 was obtained using the algorithm of Hopp and Woods (24). Above the main line are predicted hydrophilic regions and below it are hydrophobic regions. The location of the different subsequences discussed in the text are indicated. Potential glycosylation sites are indicated by closed and open circles (*O*- and *N*-linked, respectively). The leader sequences of murine eta-1 (E), human (hTR), and chicken (cTR) transferrin are shown at the left. Two potential Ca^{2+} binding sites in eta-1 (E) (positions 85–94 and 200–207) are compared with potential Ca^{2+} binding sites from thrombospondin (T) (718–727 and 769–776). The RGD-containing subsequence in eta-1 (143–149) is compared with that of fibronectin (F).

tern and sequence of the full-length *Eta-1* cDNA insert. The sequenced cDNA of 1,569 bp contained an open reading frame of 882 nucleotides (position 268–1149) that encodes a putative polypeptide with a predicted molecular mass of 32,462 daltons (Fig. 3, *B* and *C*). The first methionine in this open reading frame (positions 223–225) fits the consensus for eukaryotic translation initiation signals (21). The 3′ noncoding sequence in the cDNA contains two potential polyadenylation signals (underlined in Fig. 3 *B*) and lacks the consensus sequence "TTATTTAT" present in the mRNAs that encode other defined T cell lymphokines (22, 23).

The product of the open reading frame in the sequenced *Eta-1* cDNA is extremely hydrophilic (24) and displays several features of a secreted protein. It has a hydrophobic leader sequence that is similar to that of human and chicken transferrin (25) (Fig. 3 *C*). The leader sequence probably ends at the Ser residue at position 16 (−3,−1 rule and von Heijne's algorithm) (26, 27) almost at the transition from the NH_2-terminal hydrophobic sequence to a hydrophilic segment of the molecule (Fig. 3, *B* and *C*). The last four amino acid residues of the putative eta-1 leader sequence are similar to those in the IL-7 leader (28, 29) (Fig. 3 *C*). Eta-1 lacks an obvious membrane anchoring region (30). One potential *N*-linked glycosylation site (N-X-S or N-X-T) is present at position 78–80 (Fig. 3 C, *open circle*). There are also two tripeptides with the sequence S-X-P and 20 with the sequence S-X-E, which could serve as *O*-linked glycosylation sites (Fig. 3 C, *closed circles*). Eta-1 is unusually rich in aspartic and glutamic acid residues (22% D + E) and it has a predicted pI of 4.18.

The tripeptide sequence Arginine-Glycine-Aspartate (RGD) is present in eta-1 (Fig. 3, *B* and *C*). The RGD motif, although not unique, forms a critical part of the cellular binding site on a family of extracellular proteins that are involved in cell migration and interaction (31). The family includes fibronectin, fibrinogen, parvalbumin, thrombospondin, and vitronectin. The RGD tripeptide in eta-1 is located at residues 144–146 and is present within a longer subsequence that is highly similar to that surrounding the RGD motif in fibronectin (Fig. 3 *C*). Moreover, the RGD-containing subsequence of eta-1 contains the amino acid residues required for formation of two closely spaced β bends that determine the highly ordered structure associated with functional binding to cellular adhesion receptors (32).

There are two negatively charged stretches in eta-1 (positions 85–96 and 200–207) that are similar to subsequences in thrombospondin and are probably involved in calcium binding (Fig. 3 C and reference 33). These two subsequences are likely to constitute E-F hand calcium binding sites since most, if not all, vertex positions are occupied by aspartic acid residues (34). Calcium binding in thrombospondin has been shown to cause structural changes that may affect the specificity of binding of the adjacent RGD motif (see reference 32 for review).

Expression of Recombinant Eta-1 Protein in Mammalian Cells. To confirm that *Eta-1* cDNA is functional and that its product is secreted, COS-7m6 cells were transfected with either the pcD vector containing a full-length *Eta-1* cDNA insert (pcD-Eta-1) or the pcD vector alone (see Materials and Methods). The pcD vector includes the SV40 early enhancer-promoter region and polyadenylation signals. Poly(A)$^+$ RNA from COS-7m6 cells was obtained at 48 h after transfection and analyzed by Northern blot using radiolabeled *Eta-1* cDNA as probe (Fig. 4 *A*). The probe hybridized with a 2.2-kb RNA from COS-7m6 cells transfected with pcD-Eta-1 (Fig. 4 *A*, lane *a*) that corresponds to the expected size plus SV40 sequences. No hybridization to the

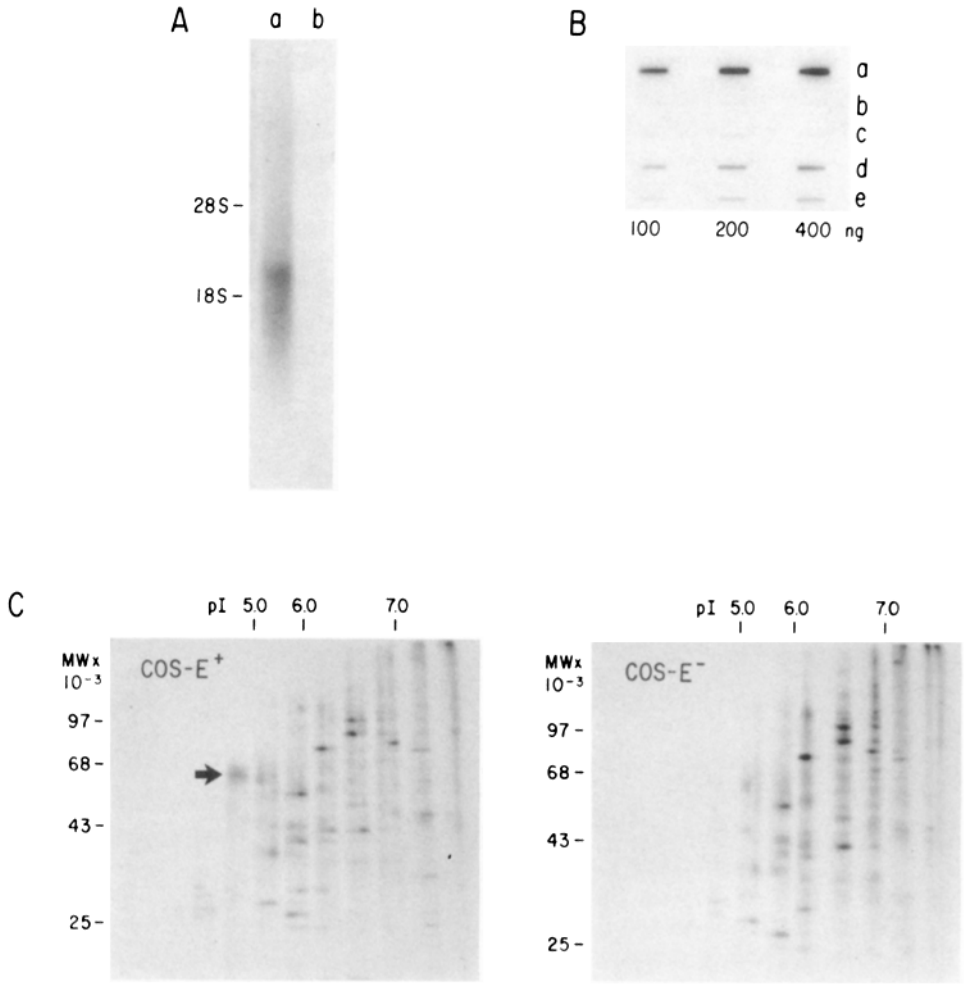

FIGURE 4. Northern and protein analysis of COS-7m6 cells transfected with pcD-Eta-1 or pcD alone. (*A*) Northern blot analysis of poly(A)$^+$ RNA obtained from COS-7m6 cells 72 h after transfection with pcD-Eta-1 (lane *a*) or with pcD alone (lane *b*). 5 μg of poly(A)$^+$ RNA was tested for *Eta-1* transcription using the nick-translated Xho I fragment as a probe (shown in Fig. 3 *A*). Hybridization (lane *a*) to a 2.2-kb RNA corresponds to the expected size of the cDNA insert (1.55 kb) plus SV40 sequences (0.5 kb) plus poly(A) (0.15 kb). (*B*) cDNA transcription increased rapidly between 48 and 72 h and decreased substantially by 96 h. This is shown by the blot analysis using the Xho I fragment as probe for total COS-7m6 cell RNA. (*a*) 72 h after transfection with pcD-Eta-1; (*b*) pcD vector without cDNA insert at 72 h; (*c*) pcD vector without insert at 80 h; (*d*) 80 h after transfection with pcD-Eta-1; and (*e*) 96 h after transfection with pcD-Eta-1. (*C*) Superantant fluid proteins from ^{35}S-methionine-labeled COS-7m6 cells that had been transfected with pcD-Eta-1 (COS-E$^+$) or pcD alone (COS-E$^-$) were analyzed by electrophoresis in two dimensions using a modification of O'Farrell (18) (see Materials and Methods). pI scale was determined by using the following standard proteins: aminoglucosidase (pH 3.55), B-lactoglobulin A (pH 5.13), and myoglobin (pH 6.76 and 7.16). The protein patterns are virtually identical except for a diffuse band having a size of ~60 kd and a pI of ~4.5 (denoted with arrow).

Eta-1 probe was detectable in RNA from COS-7m6 cells transfected with pcD vector alone (Fig. 4 *A*, lane *b*). Analysis of *Eta-1* transcription at intervals after COS cell transfection showed that maximal steady state levels of *Eta-1* RNA were present between 48 and 72 h after transfection (Fig. 4 *B*).

Two-dimensional gel electrophoresis analysis of supernatant fluids from ^{35}S metabolically labeled COS-7m6 cells that had been transfected with pcD-Eta-1 (designated as COS-E^+) or with pcD (COS-E^-) showed identical protein patterns, except for the presence in COS-E^+ of a diffuse band corresponding to a molecular mass of ~60 kD and a pI of ~4.5 (Fig. 4 *C*). Measurement of ^{35}S cpm after extraction of each of the labeled bands from the gel indicated that the 60 kD/pI 4.5 band accounted for ~5% of the total biosynthetically labeled protein in the supernatant fluid. Although the molecule migrated as a highly acidic protein, as expected from the predicted amino acid sequence of *Eta-1* cDNA, its size was larger than expected. Three independent experiments confirmed that COS-E^+ (but not COS-E^-) supernatant fluids contained a diffuse band having a pI of 4–4.5 and an estimated size of 55–60 kD (not shown). Since the secreted form of the eta-1 protein lacks cysteine residues (Fig. 3 *B*), its position on the polyacrylamide gel is not altered by cleavage of disulfide bonds. Expression of *Eta-1* cDNA in COS-7m6 cells should be accompanied by correct glycosylation. Possibly, the size of the molecule may reflect the effects of glycosylation at the sites indicated in Fig. 3 *C*, consistent with the charge heterogeneity evident after isoelectric focusing (Fig. 4 *C*). Further analysis of the protein and carbohydrate structure of this molecule is necessary for direct determination of its correspondence to the protein product predicted from the *Eta-1* cDNA sequence (Fig. 3).

Allelic Forms of Eta-1 and Linkage to the Ric Locus. To determine whether the *Eta-1* gene maps to any of the loci that are thought to affect immune responses, we determined the chromosomal location of the *Eta-1* gene using DNA from a panel of 20 mouse/hamster somatic cell hybrids. After digestion with Eco RI, a mouse-specific 6.8-kb fragment that hybridized to the radiolabeled *Eta-1* probe was either present or absent with chromosome 5 (Table I).

Digestion of DNAs from a variety of inbred strains with Eco RV (not shown) or with the combination of Eco RV and Xba I (Fig. 5) generated RFLPs that identified two *Eta-1* gene alleles (*Eta-1*^{a} and *Eta-1*^{b}) in the parental strains of the BXH and CXS series of recombinant inbred (RI) strains. Analyses of 12 BXH and 14 CXS RI strains showed complete concordance for segregation of *Eta-1* RFLPs and alleles at *Ric* (5), a locus conferring inborn resistance of mice to lethal infection with RT (Table II). Among the CXS RI strains, there was also complete concordance for *Eta-1* RFLPs and alleles at the *Afp*, *Bcd-1*, and *Dao-1* loci, which are all linked to the *Ric* locus. Additional studies of C57BL/6Ty-*le* mice were informative in placing *Eta-1* proximal to the *rd* locus in linkage with *Ric* (Table II). These results demonstrated that the *Eta-1* gene maps to chromosome 5 between the *Pgm-1* and *rd* loci, and 0–4 cM from the *Ric* locus with a confidence limit of 95% (35).

Inbred mouse strains are either very resistant (*Ric*^{R}) or very susceptible (*Ric*^{S}) to RT infection (5, 36). We asked if there was an association between expression of the two RFLPs representing *Eta-1*^{a} and *Eta-1*^{b} and the two alternative phenotypes of *Ric*. With one exception, expression of *Eta-1*^{a} was associated with the Ric^R phenotype, while expression of *Eta-1*^{b} was associated with the Ric^S phenotype (Table III).

TABLE I

Analysis of Concordance between Specific Mouse Chromosomes and the Presence of the Eta-1 Gene in a Series of Mouse-Hamster Somatic Cell Hybrids

Mouse chromosome	DNA hybridization/chromosome*				Percent discordance
	+ / +	− / −	+ / −	− / +	
1	1	4	2	9	68.8
2	2	5	1	9	58.8
3	0	7	2	6	53.3
4	1	10	2	4	35.3
5	3	13	0	0	0.0
6	1	5	2	9	64.7
7	2	2	1	12	76.5
8	1	9	2	4	37.5
9	1	9	1	5	37.5
10	0	12	3	2	29.4
11	0	9	2	0	18.2
12	1	2	1	8	75.0
13	1	5	1	8	60.0
14	0	11	3	3	35.3
15	1	0	1	10	91.7
16	1	10	1	3	26.7
17	2	3	1	11	70.6
18	2	8	1	5	37.5
19	1	8	2	5	43.8
20	1	6	2	8	58.8

* Symbols indicate the presence (+ /) or absence (− /) of the mouse *Eta-1* restriction fragment as related to the presence (/ +) of absence (/ −) of a particular mouse chromosome. The number of discordant observations is the sum of the + / − and − / + observations.

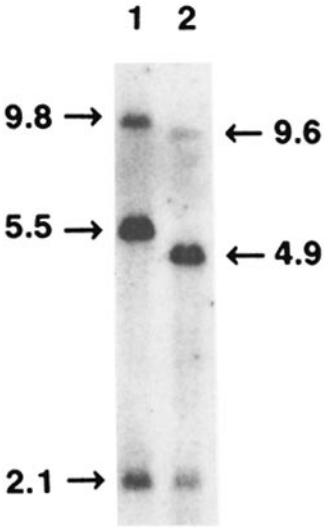

FIGURE 5. Southern blot analysis of *Eta-1* RFLP. Genomic DNA from C57BL/6 mice (lane *1*) and C3H/HeJ (lane *2*) was digested with Eco RV and Xba I, separated on agarose gels, transferred to nitrocellulose, and hybridized with ^{32}P-labeled *Eta-1* cDNA. Inbred strains with RFLPs (*Eta-1*^{a}) like C57BL/6 included BALB/cJ, BALB/cPt, BALB/cHeA, C57BL/10SnJ, CBA/CaJ, CBA/CaH-T6J, AKR/A, 020/A, DBA/2N, DBA/2J, A/J, 129/J, PL/J, SWR/J, P/J, and NZB/BINJ. Strains with patterns (*Eta-1*^{b}) like C3H/HeJ included CBA/J, C3H/HeN, STS/A, NFS/N, and SJL/J.

TABLE II

Inheritance of Eta-1 RFLP in the BxH and CxS Recombinant Inbred Mouse Strains and in the Chromosome 5 Mutant-bearing Stock C57BL/6Ty-le

	BxH											
Locus	2	3	4	6	7	8	9	10	11	12	14	19
Pgm-1	H	H	H	B	B x	H	H	B	B	B	H	H
Eta-1	H	H	H	B	H	H	H	B	B	B	H	H
Ric	H	H	H	B	H	H	H	B	B	B	H	H
rd	H x	H	H	B	H x	H	H	B x	B	B	H x	H
Gus	B	H	H	B	B	H	H	H	B	B	B	H

	CxS													
	1	2	3	4	5	6	7	8	9	10	11	12	13	14
Pgm-1	S	S	S x	S	C	C	C	C x	S x	C	C x	C x	C	C
Afp	S	S	C	S	C	C	C	S	C	C	S	S	C	C
Eta-1	S	S	C	S	C	C	C	S	C	C	S	S	C	C
Ric	S	S	C	S	C	C	C	S	C	C	S	S	C	C
Bcd-1	S	S	C	S	C	C	C	S	C	C	S	S	C	C
Dao-1	S	S	C	S	C	C	C	S	C	C	S	S	C	C
rd	S x	S x	C	S	C	C x	C	S x	C	C x	S x	S	C x	C
Gus-r	C	C	C	S	C	S	C	C	C	S	C	S	S	C

	Locus					
Strain	Pgm-1	Eta-1	Ric	rd	le	Gus
C57BL/6JTy-*le*	B	B	B x	H	H	H

The letters B, H, S, and C are used as generic symbols for the *Eta-1* RFLP of C57BL/6, C3H/HeJ, STS/A, and BALB/cHeA, respectively. The letter x indicates recombination.

Kinetics of Expression of Eta-1 in Mice after Infection with Rickettsia and Dependence on T Cells. Inbred mouse strains that carry the Ric^R (resistant) allele suppress local growth of RT after intraperitoneal inoculation, while Ric^S (susceptible) strains fail to suppress intraperitoneal growth and die from widespread infection within 10–14 d (5, 36). In view of the association of the $Eta\text{-}1^a$ RFLP with the Ric^R allele and the $Eta\text{-}1^b$ RFLP with Ric^S, we determined the levels of *Eta-1* gene expression infected with RT. CBA/CaJ and CBA/J are genetically similar substrains that differ at both *Ric* and *Eta-1*: CBA/CaJ is $Ric^R/Eta\text{-}1^a$ and CBA/J is $Ric^S/Eta\text{-}1^b$ (Table II and reference 5). *Eta-1* gene expression in peritoneal cells increased within 24 h of intraperitoneal RT infection of CBA/CaJ mice and remained elevated over the next 6 d (Fig. 6). Peritoneal cells obtained from CBA/CaJ mice 5 d after RT infection contained 0–1 RT bacterium/cell. In contrast, peritoneal cells from infected CBA/J mice did not express significant levels of *Eta-1* for the first 4 d after RT infection (Fig. 6) and peritoneal cells obtained from these mice 5 d after infection contained

TABLE III

Eta-1 Alleles and Ric Phenotypes of Different Inbred Mouse Strains

Eta-1^a/Ric^R	Eta-1^a/Ric^S	Eta-1^b/Ric^S	Eta-1^b/Ric^R
AKR/J	DBA/2J	CBA/J	-
BALB/cJ		C3H/HeJ	
CBA/CaJ		SJL/J	
CBA/CaH-T6J		STS/A	
C57BL/6J			
C57BL/10J			
P/J			
PL/J			
SWR/J			

The *Ric* phenotypes of these inbred strains are from reference 5, except for CBA/CaJ, which was determined in this study, and STS/A (J. Hilgers, personal communication). A/J mice, which show an intermediate response ("selective resistance") (36), are *Eta-1*^{a}. A contingency test (χ^2 with Yates correction) used to assess the association of *Eta-1*^{a} and *Eta-1*^{b} alleles with the *Ric*^{R} and *Ric*^{S} phenotypes, respectively, showed that this association was significant ($p < 0.05$, χ^2 = 4.48) for the independently derived mouse strains listed in the table.

>50 RT bacterium/cell. Failure to express *Eta-1*^{b} early after RT infection of CBA/J mice does not reflect a generalized failure to express this *Eta-1* allele because inoculation of these mice with Con A resulted in strong induction of *Eta-1* within 24 h (Fig. 7 *A*).

Since IFN-γ has been implicated as an important mediator of host resistance to Rickettsial infection (37, 38), we measured in situ transcription of this cytokine after

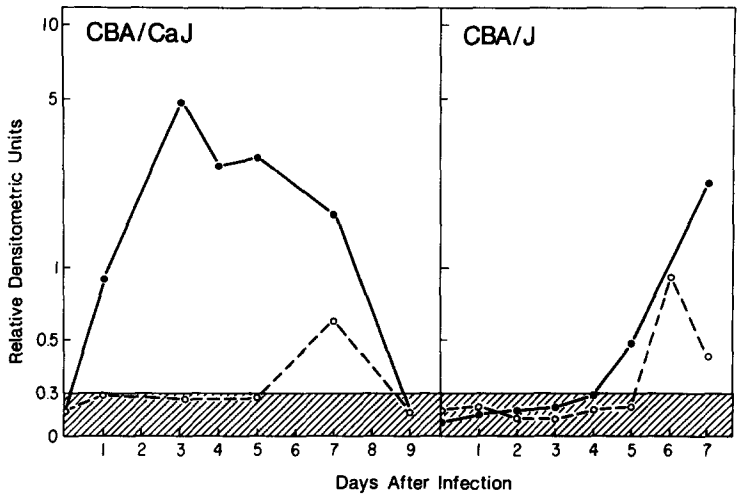

FIGURE 6. *Eta-1* and *Ifg* gene expression after RT infection of CBA/CaJ and CBA/J mice. 10^3 PFU of RT were inoculated intraperitoneally into CBA/CaJ (*left panel*) or CBA/J mice (*right panel*). The levels of steady state *Eta-1* (●) or *Ifg* (○) RNAs expressed in peritoneal cells at the indicated days after RT infection are shown. The hatched area indicates the mean +/− 2 SE of *Eta-1* and *Ifg* RDU of RNA in peritoneal cells from mice injected with saline. *Eta-1* was also elevated 3 d after RT infection of CBA/CaH-T6J mice (*Ric*^{R}/*Eta-1*^{a}), at levels similar to that of CBA/CaJ (RDU = 3.80).

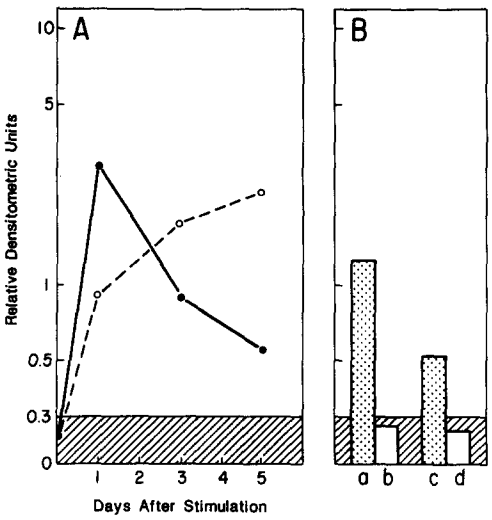

FIGURE 7. (*A*) The levels of steady state *Eta-1* RNA in peritoneal cells in CBA/J (●) and CBA/CaJ (○) are shown at different intervals after intraperitoneal injection of Con A (10 μg/mouse). (*B*) The levels of steady state *Eta-1* RNA (ordinate) in peritoneal cells 72 h after RT infection (10^3 PFU/mouse) are shown for (*a*) (CBA/J × C57BL/6)F_1 [(C × B6)F_1] euthymic mice, (*b*) (C × B6)F_1-*nu/nu* littermates, (*c*) (C × B6)F_1-*nu/nu* mice receiving 1.5 × 10^7 syngeneic splenic T cells intraperitoneally immediately before RT infection, (*d*) (C × B6)F_1-*nu/nu* mice receiving 1.5 × 10^7 syngeneic splenic Thy-1$^-$ cells intraperitoneally immediately before RT infection.

infection of the two CBA substrains. Peritoneal cells from CBA/CaJ and CBA/J mice did not express elevated levels of mRNA until 5–7 d after infection; the increase at this time was similar in the two mouse strains (Fig. 6).

Expression of *Eta-1* after T cell activation (Fig. 1) and previous studies suggesting that T cells were required for resistance to RT infection (39) prompted us to determine whether *Eta-1* induction early after RT infection depended upon T cells. (C57BL/6 × CBA/J)F_1 mice (*Ric*$^{R/S}$; *Eta-1*$^{a/b}$) expressed *Eta-1* 48 h after RT infection, consistent with the dominant effects of the *Ric*^{R} allele in conferring resistance to RT infection (Fig. 7 *B*, and reference 5). Littermates of these F_1 mice that were homozygous *nu/nu* did not express significant levels of *Eta-1* 48 h after RT infection unless they had received T cells from syngeneic donors immediately before infection (Fig. 7 *B*).

Discussion

Early protection against bacterial infection is generally thought to depend on a nonspecific host response that includes production of acute phase proteins such as complement and CRP, as well as a nonspecific reaction of macrophages and granulocytes (1). Subsequent protection comes from the development of a specific immune response that usually depends on T cells (1). This division of labor does not easily account for the host response to RT, a Gram-negative intracellular bacterium that is the etiologic agent of human scrub typhus (5). This model of bacterial infection has been studied extensively because resistance to the lethal effects of acute infection is under unigenic dominant control by the *Ric* locus (5). Susceptible mouse strains (*Ric*^{S}) allow local and systemic bacterial growth during the first week of RT infection and die within 10–12 d. By contrast, *Ric*^{R} strains show minimal levels of bacterial infection over the first week and survive infection (37, 40). Although *Ric* affects early resistance to RT infection, mice bearing the *Ric*^{R} genotype are converted to the *Ric*^{S} phenotype if T cell development is genetically impaired by the *nu* mutation (39, 41). An explanation for these observations is provided by analysis of the

Eta-1 gene, which maps to the *Ric* locus. We find that *Eta-1* expression is part of a surprisingly early T-dependent response after RT infection of Ric^R but not Ric^S hosts.

We detected *Eta-1* gene expression in activated lymphocytes, including T cells and a subset of NK cells. We have provisionally designated the gene described in these studies as *Eta-1* based upon its cellular expression in vitro and its rapid induction after RT infection in vivo. The expression of *Eta-1* by T lymphocytes and observations suggesting that it encodes a secreted product fit the definition of lymphokines and suggest that it might be given an IL prefix. However, further studies are required to determine the effect of *Eta-1* on other lymphocytes and target cells unrelated to leukocytes. In addition, a comprehensive survey of RNA from different cell types using subprobes of *Eta-1* and S1 nuclease mapping is required to completely define its cellular expression and identify potential homologous transcripts. For example, osteopontin is a bone sialoprotein that contains an RGD subsequence and is highly homologous to eta-1 (42, 43). No immunological activity for osteopontin has been shown, and osteopontin is reported to be present in bone, kidney, placenta, and certain neuronal cells (44). Osteopontin contains two additional repeats of a subsequence that is present only once in eta-1, and contains a pentapeptide, YKQRA, absent from eta-1; there are a total of 43 encoded amino acid residues that differ between eta-1 and osteopontin, out of which, 28 are nonconservative substitutions. Eta-1 shows no obvious similarity with either a recently described family of genes that may encode secreted, inducible leukocyte products (45) or with known antibacterial peptides, including attacins, cecropins, diptericins, defensins, or macrophage antibacterial products (46, 47).

Although mapping studies show complete concordance of *Eta-1* RFLP with *Ric*, it is not possible to formally demonstrate identity from coincident mapping. Additional evidence on this point comes from a survey of *Eta-1* alleles expressed by independently derived inbred mouse strains. Expression of the $Eta\text{-}1^a$ allele was associated with the Ric^R phenotype, and expression of $Eta\text{-}1^b$ was associated with the Ric^S phenotype (Table III). Independent segregation would be expected if *Ric* and *Eta-1* were closely linked but separate genes. These findings, along with its location, suggest that *Eta-1* may be the gene postulated from studies of the *Ric* locus. Direct evidence for the potential role of the *Eta-1* gene product in resistance to RT should come from the ability to transfer RT resistance by provision of recombinant eta-1 protein to genetically susceptible mouse strains.

We have so far been unable to detect additional RFLPs of the *Eta-1* gene using different restriction endonucleases. However, if the *Eta-1* gene confers resistance to RT infection, a third functional allele must be carried by DBA/2, which represents an Ric^S strain that does not express $Eta\text{-}1^b$ (Table III). Additional characterization of the structure and expression of the DBA/2 *Eta-1* gene is necessary to test this hypothesis.

We used a pair of genetically similar CBA substrains (~85–90% identical outside of *Ric* according to genetic marker analysis [48]) to study in situ expression of *Eta-1* during the course of RT infection. CBA/CaJ mice ($Eta\text{-}1^a/Ric^R$), but not CBA/J ($Eta\text{-}1^b/Ric^S$), expressed high levels of *Eta-1* throughout the first week of bacterial infection and showed minimal levels of intraperitoneal infection. These findings suggest that this form of genetic resistance may be associated with a rapid *Eta-1* response

and inhibition of early bacterial replication. Additional studies are needed to determine whether levels of eta-1 protein produced after RT infection correlate with expression at the RNA level.

The genetic mechanism resulting in differential transcriptional activation of the alleles of *Eta-1* after RT infection is not addressed in this report. Possibly, the *Eta-1*^{b} polymorphism affects an inducible segment of the gene, resulting in decreased levels of transcriptional activity after cellular activation by Rickettsia, similar to the effects of a polymorphism of the alcohol dehydrogenase gene on constitutive levels of cellular transcription (49). Alternatively, the genetic alteration in *Eta-1*^{b} may be a mutation or deletion affecting the activity of the eta-1 protein and the levels of *Eta-1* gene expression after RT infection noted in this study might reflect genetic differences outside of the *Eta-1* locus. For example, these CBA substrains also differ at *Mls-1* and *Mls-2* (50). One effect of this difference is that CBA/J, but not CBA/CaJ, mice lack a substantial population of T cells that express particular V-β chains (51). We are examining the specificity of the T cell response to RT, as well as the possibility that clonal deletion within the T cell repertoire of CBA/J mice affects the early *Eta-1* response to RT.

Although early resistance to bacterial infection has generally been attributed to nonspecific host mechanisms, there is increasing evidence that large number of T cells may be predisposed to recognize antigens expressed by some bacteria (52, 53), suggesting the possibility that infection by these bacteria might mobilize rapid and vigorous T cell responses in vivo. This appears to be the case for RT, although the mechanism of T cell activation by this bacterium is not well understood. It may be relevant that, in contrast to *Eta-1*, induction of *Ifg* is not apparent until 5–7 d after infection by RT. More sensitive methods may be required to detect an earlier increase in steady-state *Ifg* RNA. However, these data suggest that *Eta-1* expression may precede the induction of classical T cell genes in the response to this bacterial infection. Further insight into the role of this rapid T cell response in protection against bacterial infection, and its relationship to the development of classical forms of T cell immunity, should come from studies of the biological activity of the eta-1 protein.

Summary

We describe a murine cDNA, designated Early T lymphocyte activation 1 (*ETA-1*), which is abundantly expressed after activation of T cells. *Eta-1* encodes a highly acidic secreted product having structural features of proteins that bind to cellular adhesion receptors. The *Eta-1* gene maps to a locus on murine chromosome 5 termed *Ric* that confers resistance to infection by *Rickettsia tsutsugamushi* (RT), an obligate intracellular bacterium that is the etiological agent for human scrub typhus. With one exception, inbred mouse strains that expressed the *Eta-1*^{a} allele were resistant to RT infection (*Ric*^{R}), and inbred strains expressing the *Eta-1*^{b} allele were susceptible (*Ric*^{S}). These findings suggest that *Eta-1* is the gene inferred from previous studies of the *Ric* locus (5).

Genetic resistance to RT infection is associated with a strong *Eta-1* response in vivo and inhibition of early bacterial replication. *Eta-1* gene expression appears to be part of a surprisingly rapid T cell-dependent response to bacterial infection that may precede classical forms of T cell-dependent immunity.

Received for publication 22 March 1989.

References

1. Rosenstreich, D. L., A. C. Weinblatt, and A. D. O'Brien. 1982. Genetic control of resistance to infection in mice. *CRC Crit. Rev. Immunol.* 3:263.
2. Hadley, T. J., F. W. Klotz, and L. H. Miller. 1986. Invasion of erythrocytes by malaria parasites: a cellular and molecular overview. *Annu. Rev. Microbiol.* 40:451.
3. Staeheli, P., P. Danielson, O. Haller, and J. G. Sutcliffe. 1986. Transcriptional activation of the mouse *Mx* gene by type I interferon. *Mol. Cell. Biol.* 6:4770.
4. Patarca, R., G. Freeman, J. Schwartz, R. P. Singh, Q.-T. Kong, E. Murphy, Y. Anderson, F.-Y. Sheng, P. Singh, K. A. Johnson, S. M. Guarnagia, T. Durfee, F. Blattner, and H. Cantor. 1988. Rpt-1: an intracellular protein from inducer/helper T-cells that regulates gene expression of the interleukin-2 receptor and the Human Immunodeficiency Virus Type I. *Proc. Natl. Acad. Sci. USA.* 85:2733.
5. Groves, M. G., D. L. Rosenstreich, B. A. Taylor, B. A., and J. V. Osterman. 1980. Host defenses in experimental scrub typhus: mapping the gene that controls natural resistance in mice. *J. Immunol.* 125:1395.
6. Julius, M. H., E. Simpson, and L. A. Herzenberg. 1973. A rapid method for the isolation of functional thymus-derived murine lymphocytes. *Eur. J. Immunol.* 3:645.
7. Clayberger, C., R. H. DeKruyff, and H. Cantor. 1984. Immunoregulatory activities of autoreactive T-cells: an I-A specific T-cell clone mediates both help and suppression of antibody responses. *J. Immunol.* 132:2237.
8. Nabel, G., M. Fresno, A. Chessman, and H. Cantor. 1981. Use of cloned populations of mouse lymphocytes to analyze cellular differentiation. *Cell.* 23:19.
9. Clayberger, C., R. H. DeKruyff, J. Aisenberg, and H. Cantor. 1983. Hapten reactive inducer T-cells. I. Definition of two classes of hapten-specific inducer cells. *J. Exp. Med.* 157:1906.
10. Okayama, H., and P. Berg. 1983. A cDNA cloning vector that permits expression of cDNA inserts in mammalian cells. *Mol. Cell. Biol.* 3:280.
11. Shen, F. W., Y. Saga, G. Litman, G. J. Freeman, J. S. Tung, H. Cantor, and E. A. Boyse. 1985. Cloning of Ly 5 cDNA. *Proc. Natl. Acad. Sci. USA.* 82:7360.
12. Maniatis, T., E. F. Fritsch, and J. Sambrook. 1982. Molecular Cloning: A Laboratory Manual. Cold Spring Harbor Laboratory, Cold Spring Harbor, NY. 545 pp.
13. Maxam, A. M., and W. Gilbert. 1980. Sequencing end-labelled DNA with base-specific chemical cleavages. *Methods Enzymol.* 65:499.
14. Gatti, R. A., R. Conconnon, and W. Salser. 1984. Multiple use of Southern blots. *Biotechniques.* 2:148.
15. Chirgwin, J., A. E. Przbyla, R. J. MacDonald, and W. J. Rutter. 1979. Isolation of biologically active ribonucleic acid from sources enriched in ribonuclease. *Biochemistry.* 18:5294.
16. Hoggan, M. D., N. F. Halden, C. E. Buckler, and C. A. Kozak. 1988. Genetic mapping of the mouse c-fms protooncogene to chromosome 18. *J. Virol.* 62:1055.
17. Queen, C., and D. Baltimore. 1983. Immunoglobulin gene transcription is activated by downstream sequence elements. *Cell.* 33:741.
18. O'Farrell, P. H. 1975. High resolution two-dimensional electrophoresis of proteins. *J. Biol. Chem.* 250:4007.
19. Jerrells, T. R., and J. V. Osterman. 1982. Host defenses in experimental scrub typhus: delayed-type hypersensitivity responses of inbred mice. *Infect. Immun.* 35:117.
20. Piechaczyk, M., J. M. Blanchard, L. Marty, Ch. Dani, F. Panabiero, S. El Sabouty, Ph. Fort, and Ph. Jeanteur. 1984. Post-transcriptional regulation of glyceraldehyde-3-phosphate-dehydrogenase gene expression in rat tissues. *Nucleic Acids Res.* 12:6951.
21. Kozak, M. 1984. Compilation and analysis of sequences upstream from the translational start site in eukaryotic mRNAs. *Nucleic Acids Res.* 12:857.
22. Caput, D., B. Beutler, K. Hartog, R. Thayer, S. Brown-Shimer, and A. Cerami. 1986. Identification of a common nucleotide sequence in the 3'-untranslated region of mRNA

molecules specifying inflammatory mediators. *Proc. Natl. Acad. Sci. USA.* 83:1670.
23. Shaw, G., and R. Kamen. 1986. A conserved AU sequence from the 3' untranslated region of GM-CSF in RNA mediates selective mRNA degradation. *Cell.* 46:659.
24. Hopp, T., and K. Woods. 1981. Prediction of protein antigenic determinants from amino acid sequences. *Proc. Natl. Acad. Sci. USA.* 78:3824.
25. Lucero, M. A., E. Schaeffer, G. N. Cohen, and M. M. Zakin. 1986. The 5' region of the human transferrin gene: structure and potential regulatory sites. *Nucleic Acids Res.* 14:8692.
26. von Heijne, G. 1983. Patterns of amino acids near signal-sequence cleavage sites. *Eur. J. Biochem.* 133:17.
27. von Heijne, G. 1986. A new method for predicting signal sequence cleavage sites. *Nucleic Acids Res.* 14:4683.
28. Namen, A. E., S. Lupton, K. Hjerrild, J. Wignall, D. Y. Mochizuki, A. Schmierer, B. Mosley, C. J. March, D. Urdal, S. Gillis, D. Cosman, and R. G. Goodwin. 1988. Stimulation of B-cell progenitors by cloned murine interleukin-7. *Nature (Lond.).* 333:571.
29. Goodwin, R. D., S. Lupton, A. Schmierer, K. J. Hjerrild, R. Jerzy, W. Clevenger, S. Gillis, D. Cosman, and A. E. Namen. 1989. Human interleukin-7: molecular cloning and growth factor activity on human and murine B-cell lineages. *Proc. Natl. Acad. Sci. USA.* 86:302.
30. Sabatini, D. D., G. Kreibich, T. Morimoto, and T. M. Adesnik. 1982. Mechanisms for the incorporation of proteins in membranes and organelles. *J. Cell. Biol.* 92:1.
31. Ruoslahti, E., and M. D. Pierschbacher. 1986. Arg-Gly-Asp: a versatile cell recognition signal. *Cell.* 44:517.
32. Reed, J., W. E. Hull, C.-W. von der Lieth, D. Kuebler, S. Suhai, and V. Kinzel. 1988. Secondary structure of the Arg-Gly-Asp recognition site in proteins involved in cell surface adhesion. *Eur. J. Biochem.* 178:141.
33. Lawler, J., and R. Heinz. 1986. The structure of human thrombospondin, an adhesive glycoprotein with multiple calcium-binding sites and homologies with several different proteins. *J. Cell. Biol.* 103:1635.
34. Tufty, R. H., and R. H. Kretsinger. 1975. Troponin and parvalbumin calcium binding regions predicted in myosin light chain and T4 lysozyme. *Science (Wash. DC).* 187:167.
35. Silver, J. 1985. Confidence limits for estimates of gene linkage based on analysis of recombinant inbred strains. *J. Hered.* 576:436.
36. Groves, M. G., and J. V. Osterman. 1978. Host defenses in experimental scrub typhus: genetics of natural resistance to infection. *Infect. Immun.* 19:583.
37. Jerrells, T. R., and J. V. Osterman. 1982. Role of macrophages in innate and acquired host resistance to experimental scrub typhus infection of inbred mice. *Infect. Immun.* 39:1066.
38. Li, H., T. R. Jerrells, G. Spitalny and D. H. Walker. 1987. Gamma inteferon as a crucial host defense against *R. conorii* in vivo. *Infect. Immun.* 55:1252.
39. Jerrells, T. R., and C. S. Eismann. 1983. Role of T-lymphocytes in production of antibody to antigens of *Rickettsia tsutsugamushi* and other *Rickettsia species. Infect. Immun.* 41:666.
40. Nacy, C. A., and M. G. Groves. 1981. Macrophages in resistance to Rickettsial infections: early host defense mechanisms in experimental scrub typhus. *Infect. Immun.* 31:1239.
41. Murata, M., and A. Kawamura. 1977. Restoration of the infectivity of *Rickettsia tsutsugamushi* to susceptible animals by passage in a thymic nude mice-*Jpn. J. Exp. Med.* 47:385.
42. Oldberg, A., A. Franzen, and D. Heinegard. 1986. Cloning and sequence analysis of rat bone sialoprotein (osteopontin) cDNA reveals an Arg-Gly-Asp cell binding sequence. *Proc. Natl. Acad. Sci. USA.* 83:8819.
43. Franzen, A., and D. Heinegard. 1985. *In* Chemistry and Biology of Mineralized Tissues. W. T. Bolter, editor. EBSCO, Ind., Birmingham, AL. 132–141.

44. Yoon, K., R. Buenaga, and G. A. Rodan. 1987. Tissue specificity and developmental expression of rat osteopontin. *Biochem. Biophys. Res. Commun.* 148:1129.
45. Brown, K. D., S. M. Zurawski, T. R. Mosmann,and G. Zurawski. 1989. A family of small inducible proteins secreted by leukocytes are members of a new superfamily that includes leukocytes and fibroblast-derived inflammatory agents, growth factors and indicators of various activation processes. *J. Immunol.* 142:679.
46. Boman, H. G., and D. Holtmark. 1987. Cell-free immunity in insects. *Annu. Rev. Microbiol.* 41:103.
47. Lambert, J., E. Keppi, J.-L. Dimarc, C. Wicker, J.-M. Reichert, B. Dunbar, P. Lepage, A. Van Dorsselaer, J. Hoffman, J. Fothergill, and D. Hoffmann. 1989. Insect immunity: isolation from immune blood of the dipteran *Phormia terranovae* of two insect antibacterial peptides with sequence homology to rabbit lung macrophage bacteriocidal peptides. *Proc. Natl. Acad. Sci. USA.* 86:262.
48. Heiniger, H.-J., and J. J. Dorey, editors. 1980. Handbook on Genetically Standardized Jax Mice. The Jackson Laboratory, Bar Harbor, Maine.
49. Zhang, K., W. F. Bosron, and H. J. Edenberg. 1987. Structure of the mouse Adh-1 gene and identification of a deletion in a long alternating purine-pyrimidine sequence on the first intron of strains expressing low alcohol dehydrogenase activity. *Gene.* 57:27.
50. Abromson-Leeman, S., J. C. Laning, and M. E. Dorf. 1988. T cell recognition of $Mls^{c,x}$ determinants. *J. Immunol.* 140:1726.
51. Pullen, A. M., P. Marrack, and J. W. Kappler. 1988. The T-cell repertoire is heavily influenced by tolerance to polymorphic self-antigens. *Nature (Lond.).* 335:796.
52. White, J., A. Herman, A. M. Pullen, R. Kubo, J. W. Kappler, and P. Marrack. 1989. The V-beta-specific superantigen staphylococcal enterotoxin B: stimulation of mature T cells and clonal deletion in neonatal mice. *Cell.* 56:27.
53. Janeway, Jr., C. A., Y. Junji, P. J. Conrad, M. E. Katz, B. Jones, S. Vroegop, and S. Boxser. 1984. T-cell responses to Mls and to bacterial proteins that mimic its behavior. *Immunol. Rev.* 107:61.